

Two universality classes for the displacive phase transitions in perovskites

Amnon Aharony^{1,*} and Ora Entin-Wohlman^{1,†}

¹ *School of Physics and Astronomy, Tel Aviv University, Tel Aviv 6997801, Israel*

(Dated: June 13, 2022)

Perovskites like LaAlO_3 , (or SrTiO_3) undergo displacive structural phase transitions from a cubic crystal to a trigonal (or tertagonal) structure. For many years, the critical exponents in both these types of transitions have been fitted to those of the isotropic three-components Heisenberg model. Recent field theoretical accurate calculations showed that this is wrong: the isotropic fixed point of the renormalization group (RG) is unstable, and RG iterations flow either to a ‘cubic’ fixed point or to a fluctuation-driven first-order transition. These distinct flows correspond to two distinct universality classes, identified by the symmetry of the ordered structures below the transitions. Here we show that perovskites which become trigonal or tetragonal belong to these two universality classes, respectively. The close vicinity of the isotropic and cubic fixed points explains the apparent wrong observations of a single universality class, but also implies the existence of slowly varying effective material-dependent exponents. For the tetragonal case, these effective exponents can have the ‘isotropic’ values before crossing to the first-order transition. We propose dedicated experiments to test these predictions. We also expect a similar splitting of the universality classes in any situation in which two (or more) fixed points compete for stability.

Introduction.— A continuous (second-order) phase transition is accompanied by strong fluctuations of its order parameter, with a correlation length ξ which diverges as the temperature T approaches its (non-zero) critical value T_c , $\xi = \xi_0 |t|^{-\nu}$, where $t = (T/T_c - 1)$, ξ_0 is of order 1 and ν is the ‘critical exponent’ of the correlation length. (Here and below lengths, including ξ , are measured in units of the lattice constant.) The divergence of ξ implies that at T_c the system is correlated on all length scales. A similar multitude of length scales occurs, e.g., at fully developed turbulence, quantum field-theory, the Kondo effect, and the self-avoiding-walks for polymers¹. Below T_c , the n -component order parameter itself² (e.g., the magnetization of a ferromagnet, the staggered polarization of an antiferroelectric crystal, or the vector \mathbf{Q} along the rotation axis of the oxygen octahedra in the perovskites, with a magnitude proportional to the angle of rotation), which becomes non-zero at $T < T_c$, grows as $|\mathbf{Q}| \propto |t|^\beta$, with the critical exponent β . Fifty years ago, Wilson showed that at T very close to T_c the short-length details can be eliminated on scales below $1/e^\ell$ (ℓ counts the number of iterations in the elimination process), and that rescaling the unit length by the factor e^ℓ yields a renormalized effective (dimensionless) Hamiltonian $\overline{\mathcal{H}}(\ell)$, which ‘flows’ in the space spanned by all such Hamiltonians. Often this renormalization group (RG) ‘flow’ reaches the vicinity of an ℓ -independent *fixed point* (FP), $\overline{\mathcal{H}}^*$. Adding small deviations from $\overline{\mathcal{H}}^*$, $\overline{\mathcal{H}} = \overline{\mathcal{H}}^* + \sum_i \mu_i \mathcal{O}_i$, with ‘operators’ \mathcal{O}_i and ‘coupling constants’ (or ‘scaling fields’) μ_i , these scaling fields renormalize (to linear order) as $\mu_i(\ell) \approx e^{\lambda_i \ell} \mu_i(0)$. A scaling field \mathcal{O}_i is ‘relevant’ or ‘irrelevant’ when $\lambda_i > 0$ or $\lambda_i < 0$. The first two fields, which are always relevant, relate to $\mu_1(0) = t$ and to the ‘ordering field’ $\mu_2(0) = h$.

Scaling.— After $\ell = \ell_f$ iterations, the whole correlation volume reduces to one unit cell, i.e., $\xi(\ell_f) = \xi_0 |t(\ell_f)|^{-\nu} = 1$, all fluctuations have been eliminated

and simple techniques can be used to find the solution. Using $t(\ell_f) = e^{\lambda_1 \ell_f} t$, this implies that $|t(\ell_f)|$ is also of order 1, and that $\lambda_1 = 1/\nu$. The singular part of the corresponding free-energy density then obeys the homogeneous scaling form

$$\begin{aligned} \mathcal{F}(\{\mu_i\}) &= e^{-d\ell_f} \mathcal{F}(\{\mu_i(0)e^{\lambda_i \ell_f}\}) \\ &\equiv |t|^{d\nu} \mathcal{W}(h|t|^{-\nu\lambda_2}, \mu_3(0)|t|^{-\nu\lambda_3}, \dots), \end{aligned} \quad (1)$$

where d is the dimensionality. Derivatives of \mathcal{F} w.r.t. t and h yield the critical exponents for the measurable quantities, e.g. $\beta = \nu(d - \lambda_2)$. The exponents and the scaling function \mathcal{W} for systems in the corresponding universality class are fully determined by the FP itself, and not by the ‘initial’ effective Hamiltonian, which encompasses the short-scales behavior. Therefore they are ‘universal’^{3–5}.

For a ‘simple’ critical point, the other fields (μ_3, μ_4, \dots) are irrelevant, $\lambda_3, \lambda_4, \dots < 0$, decaying to zero, and the FP is ‘fully stable’. At finite $|t|$ the irrelevant fields only generate ‘corrections’ to the leading critical behavior, coming from the dependence of \mathcal{W} on the small $\mu_3(0)|t|^{\nu\lambda_3}, \mu_4(0)|t|^{\nu\lambda_4}, \dots$. In some cases, a (third) field, μ_3 , is also relevant ($\lambda_3 > 0$), yielding an RG ‘flow’ *away* from the FP, which is then ‘unstable’. Such a FP represents a ‘multicritical point’; it can be reached only if the relevant field, $\mu_3(0)$, is tuned to zero. The outcome depends on ‘initial’ parameters: the flow can go to another, ‘stable’ FP, characterizing a distinct universality class (resulting with a ‘crossover’ between these two critical behaviors⁶), or the flow does not approach any alternative FP, and $\overline{\mathcal{H}}(\ell_f)$ may yield a ‘fluctuation-driven’ first-order transition⁷. So far, there was only a limited discussion on the universality classes of such fluctuation-driven first-order transitions⁸. Below we associate such transitions with new universality classes, and discuss the critical behavior as they are approached.

Universality.— Wilson’s theory derived the FP’s from cal-

culations at $T \geq T_c$, and found a limited number of different FP's, identified by the guiding paradigm: given the interaction range (in the microscopic Hamiltonian which describes the system), the dimensionality d and the number of components of the order-parameter, n , the universality class of a FP is determined only by the *symmetry above the transition*, $T > T_c$ ^{4,5,8,9}. In the case of cubic crystals¹⁰, there exist only two FP's which can be 'fully stable', the 'isotropic' and the 'cubic' FP's (see below). Theoretically^{9,10}, it was found that the isotropic (cubic) FP is stable for $n < n_c$ ($n > n_c$), and the value of the borderline number $n_c(d)$, at $d = 3$, has been under debate. Early approximate estimates indicated that $n_c(3) > 3$, and therefore it was concluded that only the 'isotropic' FP is fully stable at $n = d = 3$, the cubic terms are irrelevant^{8,9} and all cubic systems belong to the same universality class. Below we show that this is not true.

The perovskites.— Perovskite materials exhibit intriguing physical properties, and have been extensively explored for both practical applications and theoretical modeling¹¹. At high T , perovskites usually have a cubic structure (left panel, Fig. 1). As T decreases, some perovskites undergo an antiferrodistortive structural transition from the cubic to a lower-symmetry structure, via a rotation of the oxygen (or fluorine) octahedra: SrTiO₃, KMnF₃, RbCaF₃ and others undergo a cubic to tetragonal transition, see Fig. 1. The octahedra rotate around a cubic axis and the order parameter vector \mathbf{Q} is along that axis. Similar rotations occur in double perovskites, e.g., the tetragonal to orthorhombic transition in La₂CuO₄¹². Similarly, LaAlO₃, PrAlO₃, NdAlO₃ and others undergo a cubic to trigonal transition, with \mathbf{Q} along one of the cubic diagonals.

The critical behavior of SrTiO₃ and LaAlO₃ had been measured by Müller and Berlinger¹³, who obtained a collapse of the scaled order parameters in both materials onto a single line, showing a crossover from the mean-field exponent $\beta_{MF} = 1/2$ (at relatively large $|t|$) to an apparently universal critical exponent $\beta_c = 0.33 \pm 0.02$ close to T_c . It was concluded that both materials belong to the *same universality class*. It later turned out that both samples were single domains, due to a uniaxial anisotropy caused by polishing¹⁴. Therefore both systems ordered along a *single* axis, and the data were consistent with Ising ($n = 1$) exponents^{15–17}. Later experiments are reviewed in Refs. 18–20. Although the measured exponents (e.g., β) covered some range of values, they seemed to be consistent with the 'isotropic' values, which were expected if $3 < n_c(3)$.

Our results.— Recent accurate calculations concluded that the approximate estimates were wrong, and in fact $n_c(3) < 3$ ^{21–24}, implying that the cubic fixed point is stable, and the isotropic fixed point is *unstable*, separating between the cubic FP region of 'attraction' and that of first-order transitions²⁵. Here we study physical consequences of this important conclusion. Specifically, we emphasize that, contrary to the previous conclusion, two cubic systems, which have different symmetries *below* T_c ,

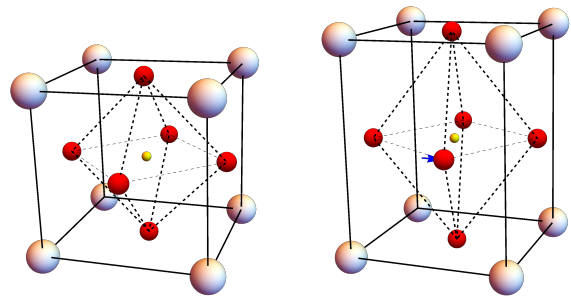


FIG. 1: (color online) The cubic (left) and tetragonal (right) unit cells in SrTiO₃ (the latter shows only half the cell: neighboring cells rotate in opposite directions). Large, intermediate and small spheres correspond to Sr, O and Ti ions, respectively. The dashed lines represent the octahedra, which rotate around the vertical axis (the O ions in the central plane move as indicated by the arrow). A rotation of the octahedra around a diagonal stretches the unit cell along that diagonal, causing a cubic to trigonal transition (as in LaAlO₃).

can belong to two different universality classes, .

For the two kinds of perovskites, we show that the cubic to trigonal transition belongs to the universality class of the cubic FP. In contrast, the cubic to tetragonal transition first (at intermediate $|t|$'s) exhibits critical exponents from the vicinity of the unstable 'isotropic' FP, but eventually (close to T_c) undergoes a 'fluctuation-driven' first-order transition. The latter behavior applies to *all* the cubic to tetragonal transitions, and can thus be associated with a separate universality class. We suggest that other fluctuation-driven first-order transitions can also be identified by universality classes, associated with their symmetry below T_c . This suggestion, and the splitting of universal critical phenomena into separate low- T symmetry determined universality classes, is our main result.

Numerically, the two competing FP's at $n = d = 3$ are close^{21–24}, and it would seem difficult to differentiate between them. This may explain the false apparent universality between the two kinds of perovskites, seen in some experiments. Below we show that the RG flows in the vicinity of both FP's are slow, and therefore they exhibit 'effective' exponents (which depend on the range of t , see below). We propose dedicated measurements of these exponents to test the different critical behaviors predicted here, and list examples of other phase transitions which may require similar renewed analyses.

The Wilson-Fisher Renormalization group.— Ignoring fluctuations, phase transitions are described by a Landau expansion of the free-energy density in powers of the (small) order parameter components Q_i . The terms in this expansion are based on the symmetries of the system above the transition²⁶. For the isotropic n -component order parameter vector \mathbf{Q} , this free-energy is $U_0(\mathbf{Q}) = r|\mathbf{Q}|^2/2 + u|\mathbf{Q}|^4 + \mathcal{O}[|\mathbf{Q}|^6]$, where $r \propto t$ and u is a system-dependent parameter. In the cubic case this should be supplemented by $U_v(\mathbf{Q}) = v \sum_{i=1}^n Q_i^4$, with v

a system-dependent coefficient^{10,27}. Long wave-length fluctuations in $\mathbf{Q}(\mathbf{r})$ are introduced via a gradient term, $|\nabla\mathbf{Q}(\mathbf{r})|^2$, whose coefficient is normalized to 1. The effective Hamiltonian is then written as $\int d^d r \bar{\mathcal{H}}(\mathbf{r})$, where

$$\bar{\mathcal{H}}(\mathbf{r}) \equiv |\nabla\mathbf{Q}(\mathbf{r})|^2/2 + U_0[\mathbf{Q}(\mathbf{r})] + U_v[\mathbf{Q}(\mathbf{r})], \quad (2)$$

with $\mathbf{Q}(\mathbf{r})$ and $\nabla\mathbf{Q}(\mathbf{r})$ generating the ‘operators’ discussed above. For $v = 0$, the Wilson-Fisher RG at $d = 4 - \epsilon$ gives^{3,28} two FP’s, one at $u_G^* = 0$, termed ‘Gaussian’, and the ‘isotropic’ FP, with $u_I^*(n) = \mathcal{O}[\epsilon] > 0$. The Gaussian FP is unstable, so that $u > 0$ flows to the isotropic FP⁶ and $u < 0$ flows to a region with a first-order transition (stabilized by the sixth order terms)⁷. The Gaussian FP is thus identified as a ‘tricritical point’. *Cubic systems.*— The RG analysis of the cubic model, Eq. (2), for general n and in dimension $d = 4 - \epsilon$ ^{10,29,30} yielded four FP’s of order ϵ : the Gaussian (G, $u_G^* = v_G^* = 0$), isotropic (I, $v_I^* = 0$, $u_I^* > 0$), decoupled Ising (D, $u_D^* = 0$, $v_D^* > 0$, for which the different Q_i ’s decouple from each other), and ‘cubic’ FP’s. The location of the cubic FP, (u_C^*, v_C^*) , depends on n : for small (large) n , it is in the lower (upper) half plane, as shown on the left (right) panel of Fig. 2. This figure⁹ has been reproduced by other authors, e.g., Refs. 22,23,25, using various methods, and included in textbooks³¹. It shows the ‘critical surface’ of the effective Hamiltonian in the $u - v$ plane, on which $|t| = 0$ and $\xi = \infty$ ³². At a finite (but very small) $|t|$ the RG flow starts very close to this surface, and as the RG is iterated the flow stays close to the arrows in the figure. When the flow reaches the vicinity of a FP the system exhibits the critical exponents of that FP.

As seen in Fig. 2, the Gaussian FP is doubly unstable; both u and v are relevant in its vicinity. The decoupled FP is singly unstable, with u relevant^{9,33}. As mentioned, the stability of the isotropic and cubic FP’s depends on the borderline value $n_c(3)$. It was clear that $2 < n_c(3) < 4$, but different approximations yielded conflicting answers to the question whether $n = d = 3$ is above or below $n_c(3)$ (for the history, see Refs. 17,21–25 and references therein). For instance, a third-order ϵ -expansion gave⁹ $n_c(3) \approx 3.128$ at $\epsilon = 1$. The result $3 < n_c(d = 3)$ was also obtained by the scaling-field method³⁴. Accepting this result, the RG flows are those shown on the left panel of Fig. 2.

We now show that when $3 < n_c(d = 3)$, both families of perovskites belong to the same universality class. At $T < T_c$, $|\mathbf{Q}|$ becomes non-zero. For the isotropic case, with $v = 0$, \mathbf{Q} can point in arbitrary directions. However, U_v breaks this symmetry. It is minimized (at $\ell = \ell_f$) for \mathbf{Q} along a cubic axis (tetragonal) when $v < 0$ and for \mathbf{Q} along a cubic diagonal (trigonal) when $v > 0$. As can be seen from the trajectories in Fig. 2, the RG iterations preserve these symmetries and the sign of v does not change under them. Therefore, we conclude that for the cubic to tetragonal (trigonal) transition, the ‘initial’ effective Hamiltonian *must* be in the lower (upper) half plane. For $n < n_c(3)$, the region of attraction of the

isotropic FP (shaded area on the left panel in Fig. 2) contains flows with both signs of v , and therefore one would conclude that the two types of transition belong to the *same* universality class, of the ‘isotropic’ FP.

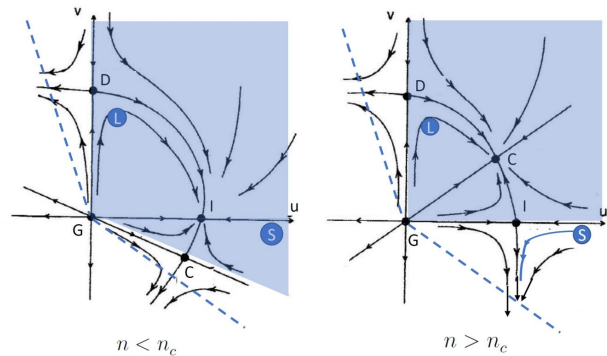


FIG. 2: (color online) Schematic flow diagram and FP’s for the cubic model, Eq. (2), adapted from Ref. 9. G=Gaussian, I=isotropic, D=Decoupled (Ising) and C=Cubic FP’s. S=initial point for SrTiO₃. L=initial point for LaAlO₃. The dashed lines represent the stability edges, $u+v=0$ (for $v < 0$) and $u+v/n=0$ (for $v > 0$), below which the free energy in Eq. (2) is stabilized by the terms of order $|\mathbf{Q}|^6$, and the transitions are first-order. The shaded areas are the regions of attraction of the stable FP’s (I on left and C on right).

As opposed, four very accurate methods (Monte Carlo simulations of lattice O(n) models²¹, six-loop recursion relations²² at $d = 3$, the good old ϵ -expansion²³ to order ϵ^6 and the bootstrap method, which calculates exponents at any dimension²⁴) find $2.85 < n_c(3) < 3$. Therefore, the RG flows are as in the right panel in Fig. 2: the isotropic FP is *unstable* [with a small but positive exponent for the ‘flow’ of v , $0 < \lambda_v^I \simeq 0.02$, see Eq. (1)], while the cubic FP has a small but positive FP value $v_C^* > 0$, and is fully stable (deviations of both u and v from it decay under iterations).

Without even looking at the specific numerical values of the locations of the FP’s, the right panel of Fig. 2 yields *qualitative* crucial consequences: since the cubic to trigonal and cubic to tetragonal transitions correspond to opposite signs of v , they have different flow trajectories. For the former, $v < 0$. If the initial $|v|$ is small, and if the initial u is positive, so that $u+v > 0$, then the respective effective Hamiltonian (shown by the blue trajectory leaving S in Fig. 2) first ‘flows’ closer to the isotropic FP, and may then exhibit t -dependent effective exponents associated with that FP, but eventually it *must* turn downwards, and cross the stability line $u+v=0$ - turning the transition fluctuation-driven first-order³⁵. As λ_v^I is small at $n = d = 3$,^{21–24} this flow is slow, so that the first-order transition will occur only close to T_c , with a small discontinuity. For larger initial $|v|$ ’s the transition becomes first-order at larger $|t|$. In contrast, the cubic to trigonal transition has $v > 0$, and therefore its Hamiltonian *must* flow to the stable cubic FP, resulting in a second-order transition with cubic exponents.

As mentioned above, the cubic and the isotropic FP’s

are close to each other at $n = d = 3$ ^{21–24}. Indeed, the calculated ‘asymptotic’ critical exponents (expected only at very small $|t|$) are $\nu_I \simeq 0.706$, $\nu_C \simeq 0.700$, $\beta_I \simeq 0.366$, $\beta_C \simeq 0.368$. This closeness also implies that the stability exponent of the stable cubic FP, $\lambda_3^C \lesssim 0$ and that of the unstable isotropic FP, $\lambda_v^I \gtrsim 0$, are small, indicating slow flows towards and away from these FP’s. The experimental exponent should therefore be compared with ‘effective exponents’, e.g., $\beta_{\text{eff}} \equiv \partial \log |\mathbf{Q}| / \partial \log |t|$, which depend on $|t|$. For $v > 0$, the cubic FP is stable, with two negative stability exponents, $\lambda_1^C < \lambda_2^C < 0$. Therefore β_{eff} approaches the asymptotic β_C slowly, with corrections of order $|t|^{|\phi_2^C|}$, where $\phi_2^C = \nu_C \lambda_2^C$ is small. For $v < 0$, β_{eff} first approaches the isotropic FP value β_I (with the relatively large exponent $|\phi_u^I|$, but then (for smaller $|t|$, i.e. larger ℓ), it moves away from that value, and $|\mathbf{Q}|$ has a discontinuity. We expect that dedicated experiments, deducing the effective exponents from various ranges of $|t|$, will corroborate these predictions³⁶.

Experiments on the perovskites.—Based on the mean-field region of the experiments, Müller *et al.*³⁷ estimated the ‘initial’ Landau parameters to be $\{u, v\}_S \cong \{1.91, -0.068\}$ for SrTiO₃ and $\{u, v\}_L \cong \{0.06 \pm 0.06, 0.68 \pm 0.06\}$ for LaAlO₃, all in cgs units divided by 10⁴³. These rough values (which should be improved!) fit beautifully with our expectations: SrTiO₃ (S in Fig. 2) has a small negative v , and we predict that it should flow near the isotropic FP before turning slowly towards first-order, while LaAlO₃ (L in Fig. 2) should flow slowly towards the cubic FP. Indeed, we found no experiments showing first-order transitions into the trigonal phase, but several experiments found such transitions into the tetragonal phase. First, some experiments hint that SrTiO₃ may be close to a tricritical point^{38–40}. Also, both RbCaF₃ and KMnF₃ have first-order transitions^{41,42}, confirming our theoretical expectations. All these systems exhibit intermediate regions with effective critical exponents [$\beta \simeq 0.40 \pm 0.03$, $1/3$, 0.27 , 0.17 ± 0.02 for SrTiO₃⁴³, KMnF₃⁴⁴, RbCaF₃ and NaNbO₃⁴⁵, respectively]. The latter smaller values have also been attributed to the inter-plane weak correlations along the rotation axis⁴⁶.

Uniaxial stress.—Frequently experimenters apply a uniaxial stress, g , which ‘prefers’ ordering along a single direction (or perpendicular to it). Such a perturbation is relevant near both the isotropic and cubic FP’s, scaling as $g(\ell) = g(0)e^{\lambda_g \ell}$ with $\lambda_g > 0$ and yielding a crossover to a uniaxial or a transverse ordering^{14,16}. The scaling function \mathcal{W} in Eq. (1) also depends on $g/|t|^{\phi_g}$, with the ‘uniaxial anisotropy exponent’ $\phi_g = \nu \lambda_g$ ⁴⁷. As $|t|$ decreases, $\mathcal{W}(g/|t|^{\phi_g})$ becomes singular at some constant parameter $g/|t|^{\phi_g} = y_0$, indicating the lower symmetry transition when $T_c(g) - T_c(0) \sim g^{1/\phi_g}$. Experiments with stress along the ‘easy axes’ [100] on SrTiO₃ and [111] on LaAlO₃ were fitted to this form with $\phi_g = 1.27 \pm 0.06$ ⁴⁸ and $\phi_g = 1.31 \pm 0.07$ ³⁷, in apparent agreement with the ‘joint’ asymptotic isotropic-cubic value 1.27. Similar

values of ϕ_g also came from elastic measurements: since $\mathcal{F} = |t|^{d\nu} \mathcal{W}(g/|t|^{\phi_g})$, the strains scale as $e_{ij} \sim |t|^{d\nu - \phi_g}$, and the elastic compliance diverges as $|t|^{d\nu - 2\phi_g}$ ¹⁴. So far, experiments gave inconclusive results concerning universality⁴⁹, and more experiments are needed⁵⁰.

Mixed crystals.—One way to vary v experimentally is to use mixed crystals, e.g. Sr_{1-x}Ca_xTiO₃⁵¹ or a mixture of SrTiO₃ with LaAlO₃, which should be easy to grow due to their matching lattice constants⁵². Since both the isotropic and cubic FP’s have $d\nu > 2$, randomness is irrelevant⁵³ and one should see the same competition predicted above.

Other $n = 3$ systems.—Three-component order parameter vectors \mathbf{Q} with cubic symmetry are abundant. Examples include ferroelectric transitions from cubic to tetragonal or trigonal, ferromagnets and antiferromagnets with the magnetization ordering along an axis or a diagonal. In particular, our results should apply to the uniaxial antiferromagnets in a parallel magnetic field [which ‘cancels’ the anisotropy to yield a (cubic or isotropic) point with $n = 3$]^{16,54}. Close to their transitions, these cubic crystals may be described by Eq. (2), and therefore their critical behavior should split into the two universality classes described above. In particular, *ordering of the $n = 3$ cubic system along a cube axis must be fluctuation-driven first-order, with intermediate effective isotropic exponents!* This important prediction should be tested experimentally⁵⁵.

Competing order parameters.—Systems having two competing order parameters, \mathbf{Q}_1 and \mathbf{Q}_2 , with n_1 and n_2 components [e.g. an Ising ferromagnet ($n_1 = 1$) and an incommensurate spin density wave with a complex order parameter which can be described by an $n_2 = 2$ model, or an isotropic antiferromagnet ($n_1 = 3$) and a superconductor ($n_2 = 2$)⁵⁶], with $n = n_1 + n_2$, are often described by replacing the quartic terms in Eq. (2) by⁵⁴

$$U_b = u_1 |\mathbf{Q}_1|^4 + u_2 |\mathbf{Q}_2|^4 + 2w |\mathbf{Q}_1| |\mathbf{Q}_2|^2. \quad (3)$$

As before, the isotropic FP $u_1 = u_2 = w$ is stable for $n < n_c$. New accurate calculations^{57,58} show that for $n = 3$ this FP is unstable, and another FP (called ‘biconical’, with all three coefficients being non-zero) becomes stable. The flow diagram is similar to the right panel in Fig. 2: Hamiltonians with $w^2 \geq u_1 u_2$, which have separate ordered phases of \mathbf{Q}_1 or of \mathbf{Q}_2 , flow to the vicinity of the isotropic FP, and then yield first-order transitions. On the other hand, Hamiltonians with $w^2 < u_1 u_2$ flow to the biconical FP (which replaces the cubic FP in our discussion). As in our cubic example, we predict that initial Hamiltonians on the two sides of the isotropic FP line belong to different universality classes. In contrast, for $n \geq 4$ there exists an exact scaling argument^{9,33}, which shows that the stable fixed point is always decoupled, i.e., $w_D^* = 0$. For modern examples, see Ref. 59. We shall elaborate on all these examples in a separate paper.

Conclusions.—In conclusion, we have shown the breakdown of the assumption that universality is determined

by the symmetry above the transition. We also identified new universality classes, which depend on the symmetry below the transition, but then have a fluctuation-driven first-order transition. This resolves a long standing confusion about the displacive phase transitions in the perovskites, and leaves its complete confirmation to future dedicated experiments, concentrating on the t -dependence of the effective exponents. We expect similar phenomena in other cases with competing fixed points. As we showed, symmetry below the transition (e.g., tetragonal) is sufficient to predict a fluctuation-driven first-order

transition.

Acknowledgments

This research was initiated by a very stimulating discussion with Slava Rychkov, who drew our attention to the new accurate values of n_c (see also Ref. 17). We also thank Andrej Kudlis for help on Ref. 23. This work is supported by the Pazy Foundation.

-
- * Electronic address: aaharonyaa@gmail.com
 † Electronic address: orawohlman@gmail.com
- ¹ K. G. Wilson, *The renormalization group and critical phenomena* (1982, Nobel Prize Lecture), *Rev. Mod. Phys.* **55**, 583 (1983).
 - ² An n -component vector order parameter describes uniaxial, easy plane or fully rotationally invariant magnets (modeled by the Ising model, $n = 1$, the XY-model, $n = 2$, or the Heisenberg model, $n = 3$). Such vectors also describe ferroelectric and other displacive phase transitions. $n = 1$ also represents e.g., simple fluids and binary mixtures, $n = 2$ also represents e.g., some incommensurate wave systems, and liquid crystals. Many models with $n > 3$ are listed in Ref. 8. Other examples include quark-gluon plasma in some models of quantum chromodynamics ($n = 4$), neutron star matter ($n = 10$) and superfluid Helium-3 ($n = 18$). All of these require deviations from the isotropic limit, as we discuss.
 - ³ K. G. Wilson and J. Kogut, *The renormalization group and the ϵ expansion*, *Phys. Rep.* **12**, 75 (1974).
 - ⁴ M. E. Fisher, *The renormalization group in the theory of critical behavior*, *Rev. Mod. Phys.* **46**, 597 (1974).
 - ⁵ M. E. Fisher, *Renormalization group theory: Its basis and formulation in statistical physics*, *Rev. Mod. Phys.* **70**, 653 (1998).
 - ⁶ e.g., A. D. Bruce and D. J. Wallace, *Crossover behaviour and effective critical exponents in isotropic and anisotropic Heisenberg systems*, *J. Phys. A: Math. Gen.* **9**, 1117 (1976).
 - ⁷ J. Rudnick and D. R. Nelson, *Equations of state and renormalization-group recursion relations*, *Phys. Rev. B* **13**, 2208 (1976); J. Rudnick, *First-order transition induced by cubic anisotropy*, *Phys. Rev. B* **18**, 1406 (1978); D. Blankschtein and A. Aharony, *Crossover from Fluctuation-Driven Continuous Transitions to First-Order Transitions*, *Phys. Rev. Lett.* **47**, 439 (1981).
 - ⁸ J.-C. Toledano, L. Michel, P. Toledano, and E. Brézin, *Renormalization-group study of the fixed points and of their stability for phase transitions with four-component order parameters*, *Phys. Rev. B* **31**, 7171 (1985).
 - ⁹ A. Aharony, *Dependence of universal critical behavior on symmetry and range of interaction*, in **Phase Transitions and Critical Phenomena**, C. Domb and M. S. Green, eds., Vol. 6 (Academic Press, NY, 1976), pp. 357-424.
 - ¹⁰ A. Aharony, *Critical behavior of anisotropic cubic systems*, *Phys. Rev. B* **8**, 4270 (1973).
 - ¹¹ F. Dogan, H. Lin, M. Guilloux-Viry and O. Peña, *Focus on properties and applications of perovskites*, *Sci. Technol. Adv. Mater.* **16**, 020301 (2015).
 - ¹² J. D. Axe and M. K. Crawford, *Structural instabilities in lanthanum cuprate superconductors*, *J. Low Temp. Phys.* **95**, 271 (1994).
 - ¹³ K. A. Müller and W. Berlinger, *Static critical exponents at structural phase transitions*, *Phys. Rev. Lett.* **26**, 13 (1971).
 - ¹⁴ A. Aharony and A. D. Bruce, *Polycritical points and flop-like displacive transitions in Perovskites*, *Phys. Rev. Lett.* **33**, 427 (1974).
 - ¹⁵ K. A. Müller and W. Berlinger, *Behavior of SrTiO₃ near the [100]-stress-temperature bicritical point*, *Phys. Rev. Lett.* **35**, 1547 (1975).
 - ¹⁶ A. D. Bruce and A. Aharony, *Coupled order parameter, symmetry breaking irrelevant scaling fields and tetracritical points*, *Phys. Rev. B* **11**, 478 (1975).
 - ¹⁷ The history of the interplay between theory and experiments following this exchange, and a preliminary report of the present results, were recently reviewed in three lectures by A. Aharony, at **Bootstat 2021: Conformal Bootstrap and Statistical models**, Paris, May 2021.
 - ¹⁸ R. Pynn and A. Skjeltorp, eds., **Multicritical Phenomena**, Proc. NATO advanced Study Institute series B, Physics; Vol. 6, Plenum Press, NY 1984.
 - ¹⁹ K. A. Müller and H. Thomas, eds., **Structural phase transitions I**, and **Structural phase transitions II** (Springer-Verlag Berlin, 1991).
 - ²⁰ R. A. Cowley, *The Phase Transition of Strontium Titanate*, *Phil. Trans.: Math., Phys. and Eng. Sci.* **354**, 2799 (1996).
 - ²¹ M. Hasenbusch and E. Vicari, *Anisotropic perturbations in three-dimensional $O(N)$ -symmetric vector models*, *Phys. Rev. B* **84**, 125136 (2011).
 - ²² J. M. Carmona, A. Pelissato and E. Vicari, *N -Component Ginzburg-Landau Hamiltonians with cubic anisotropy: A six-loop study*, *Phys. Rev. B* **61**, 15136 (2000).
 - ²³ L. T. Adzhemyan, E. V. Ivanova, M. V. Kompaniets, A. Kudlis, and A. I. Sokolov, *Six-loop ϵ expansion study of three-dimensional n -vector model with cubic anisotropy*, *Nucl. Phys. B* **940**, 332 (2019). The detailed coefficients of the ϵ expansions appear in the Ancillary files of [arXiv:1901.02754](https://arxiv.org/abs/1901.02754).
 - ²⁴ S. M. Chester, W. Landry, J. Liu, D. Poland, D. Simmons-Duffin, N. Su and A. Vichi, *Bootstrapping Heisenberg magnets and their cubic anisotropy*, [arXiv:2011.14647](https://arxiv.org/abs/2011.14647).
 - ²⁵ A. Pelissetto and E. Vicari, *Critical phenomena and renormalization-group theory*, *Phys. Rep.* **368**, 542 (2002).
 - ²⁶ L. D. Landau and E. M. Lifshitz, **Statistical Physics**,

- (Pergammon, 1994).
- ²⁷ J. C. Slonczewski and H. Thomas, *Interaction of Elastic Strain with the Structural Transition of Strontium Titanate*, *Phys. Rev. B* **1**, 3599 (1970).
- ²⁸ K. G. Wilson and M. E. Fisher, *Critical Exponents in 3.99 Dimensions*, *Phys. Rev. Lett.* **28**, 240 (1972), K. G. Wilson, *Feynman-Graph Expansion for Critical Exponents*, *Phys. Rev. Lett.* **28**, 548 (1972).
- ²⁹ R. A. Cowley and A. D. Bruce, *Application of the Wilson theory of critical phenomena to a structural phase transition*, *J. Phys. C: Solid State Phys.* **6**, L191 (1973).
- ³⁰ I. J. Ketley and D. J. Wallace, *A modified ϵ expansion for a hamiltonian with cubic point-group symmetry*, *J. Phys. A: Math. Nucl. Gen.* **6**, 1667 (1973).
- ³¹ e.g. P. M. Chaikin and T. C. Lubensky, **Principles of Condensed Matter Physics**, (Cambridge University Press, 1995); J. Cardy, **Scaling and Renormalization in Statistical Physics**, (Cambridge University press, 1996); M. Kardar, **Statistical physics of fields**, (Cambridge University press 1997).
- ³² At $t = 0$, $\xi = \infty$, and the flow stays on the $u - v$ plane. For a finite sample, the cutoff ξ in Eq. (1) is replaced by the system's linear size, L . Macroscopic quantities, like the average order-parameter, are then powers of L , e.g. $|\mathbf{Q}| \propto L^{-\beta/\nu}$. This is the basis for finite-size scaling.
- ³³ A. Aharony, *Old and new results on multicritical points*, *J. Stat. Phys.* **110**, 659 (2003).
- ³⁴ E. Domany and E. K. Riedel, *Study of cubic anisotropy in three dimensions by the scaling-field method*, *J. of Appl. Phys.* **50**, 1804 (1979).
- ³⁵ E. Domany and M. E. Fisher, *Equations of state for bicritical points. III. Cubic anisotropy and tetracriticality*, *Phys. Rev. B* **15**, 3510 (1977).
- ³⁶ A detailed quantitative analysis of this situation will appear elsewhere: A. Aharony, O. Entin-Wohlman and A. Kudlis, unpublished.
E. Domany, D. Mukamel, and M. E. Fisher, *Destruction of first-order transitions by symmetry-breaking fields*, *Phys. Rev. B* **15**, 5432 (1974). See also
- ³⁷ K.A. Müller, W. Berlinger, J.E. Drumheller and J.G. Bednorz, *Bi- and Tetra-critical Behaviour of Uniaxially Stressed LaAlO₃*, in Ref. 18, p. 143.
- ³⁸ P. R. Garnier, *Specific heat of SrTiO₃ near the structural transition*, *Phys. Lett.* **35A**, 413 (1971).
- ³⁹ J. O. Fossum, K. Fossheim and H. J. Scheel, *Ultrasonic investigation of the phase transition in flux-grown SrTiO₃*, *Solid State Comm.* **51**, 839 (1984).
- ⁴⁰ E. K. H. Salje, M. C. Gallardo, J. Jiménez, F. J. Romero and J. del Cerro, *The cubic-tetragonal phase transition in strontium titanate: excess specific heat measurements and evidence for a near tricritical, mean field type transition mechanism*, *J. Phys.: Condens. Matter* **10**, 5535 (1998).
- ⁴¹ M. Hikada, S. Maeda and J. S. Storey, *Structural phase transitions of RbCaF₃*, *Phase Transitions* **5**, 219 (1985).
- ⁴² S. Stokka and K. Fossheim, *Specific heat and phase diagrams for uniaxially stressed KMnF₃*, *J. Phys. C: Solid State Phys.* **15**, 1161 (1982).
- ⁴³ K.A. Müller and J. C. Fayet, *Structural phase transitions studied by electron paramagnetic resonance*, in Ref. 19, Vol. II, p. 1.
- ⁴⁴ F. Borsa and A. Rigamonti, *Comparison of NMR and NQR studies of phase transitions in disordered and ordered crystals*, in Ref. 19, Vol. II, p. 83.
- ⁴⁵ G. O'Ariano, S. Aldrovandi, and A. Rigamonti, *Critical behavior of the order parameter at antiferrodistortive transitions with cubic fluctuations*, *Phys. Rev. B* **25**, 7044 (1982).
- ⁴⁶ A. Aharony and A. D. Bruce, *Lifshitz-point critical and tricritical behavior in anisotropically stressed perovskites*, *Phys. Rev. Lett.* **42**, 462(1979) and references therein; J. Y. Buzaré, J. C. Fayet, W. Berlinger and K. A. Müller, *Tricritical behavior of uniaxially stressed RbCaF₃*, *Phys. Rev. Lett.* **42**, 465 (1979) Similar phenomena were also observed for uniaxially stressed KMnF₃ [S. Stokka and K. Fossheim, *Specific heat and phase diagrams for uniaxially stressed KMnF₃*, *J. Phys. C: Solid State Phys.* **15**, 1161 (1982)].
- ⁴⁷ M. E. Fisher and P. Pfeuty, *Critical behavior of the anisotropic n -vector model*, *Phys. Rev. B* **6**, 1889 (1972); P. Pfeuty, D. Jasnow, and M. E. Fisher, *Crossover scaling functions for exchange anisotropy*, *Phys. Rev. B* **10**, 2088 (1974).
- ⁴⁸ S. Stokka and K. Fossheim, *Crossover exponent and structural phase diagram of SrTiO₃*, *Phys. Rev. B* **25**, 4896 (1982).
- ⁴⁹ U. T. Höchli and A. D. Bruce, *Elastic critical behaviour in SrTiO₃*, *J. Phys. C: Solid State Phys.* **13** 1963 (1980).
- ⁵⁰ The uniaxial anisotropy exponents for the cubic FP differ for stress along an axis or along a diagonal, see A. Aharony, *Axial and diagonal anisotropy crossover exponents for cubic systems*, *Phys. Lett.* **59A**, 163 (1976).
- ⁵¹ B. S. de Lima *et al.*, *Interplay between antiferrodistortive, ferroelectric and superconducting instabilities in Sr_{1-x}Ca_xTiO_{3- δ}* , *Phys. Rev. B* **91**, 045108 (2015).
- ⁵² As emonstrated by the hetero-interface between the two materials, see A. Ohtomo and H. Hwang, *A high-mobility electron gas at the LaAlO₃/SrTiO₃ heterointerface*, *Nature* **427**, 423 (2004).
- ⁵³ A. B. Harris, *Effect of random defects on the critical behaviour of Ising models*, *J. Phys. C: Solid State Phys.* **7**, 1671 (1974). See also A. Aharony, *Critical behavior of amorphous magnets*, *Phys. Rev. B* **12**, 1038 (1982).
- ⁵⁴ J. M. Kosterlitz, D. R. Nelson and M. E. Fisher, *Bicritical and tetracritical points in anisotropic antiferromagnetic systems*, *Phys. Rev. B* **13**, 412 (1976).
- ⁵⁵ The distinction between ordering along an axis or along a diagonal was already noticed in Ref. 25. Here we emphasise the universality of the former, and the isotropic-like effective exponents for this universality class.
- ⁵⁶ E. Demler, W. Hanke, and S.-C. Zhang, *SO(5) theory of antiferromagnetism and superconductivity*, *Rev. Mod. Phys.* **76**, 909 (2004).
- ⁵⁷ P. Calabrese, A. Pelissetto, and E. Vicari, *Multicritical phenomena in $O(n_1) \oplus O(n_2)$ -symmetric theories*, *Phys. Rev. B* **67**, 054505 (2003).
- ⁵⁸ R. Folk, Yu. Holovatch, and G. Moser, *Field theory of bicritical and tetracritical points. I. Statics*, *Phys. Rev. E* **78**, 041124 (2008).
- ⁵⁹ E. Fradkin, S. A. Kivelson, and J. M. Tranquada, *Colloquium: Theory of intertwined orders in high temperature superconductors*, *Rev. Mod. Phys.* **87**, 457 (2015).